HHS Public Access

Author manuscript

Med Biol Eng Comput. Author manuscript; available in PMC 2021 April 01.

Published in final edited form as:

Med Biol Eng Comput. 2020 April ; 58(4): 739–751. doi:10.1007/s11517-020-02120-0.

Estimating total maximum isometric force output of trunk and hip muscles after spinal cord injury

Akhil Bheemreddy[1,2], **Aidan Friederich**[1,2], **Lisa Lombardo**[2], **Ronald J. Triolo**[1,2,3], **Musa L. Audu**[1,2]

[1]Department of Biomedical Engineering, Case Western Reserve University, Cleveland, OH, USA

[2]Motion Study Laboratory, Louis Stokes Cleveland Department of Veterans Affairs Medical Center, Cleveland, OH 44106, USA

[3]Department of Orthopedics, Case Western Reserve University, Cleveland, OH, USA

Abstract

Functional neuromuscular stimulation (FNS) can be used to restore seated trunk function in individuals paralyzed due to spinal cord injury (SCI). Musculoskeletal models allow for the design and tuning of controllers for use with FNS; however, these models often use aggregated estimates for parameters of the musculotendon elements, the most significant of which is maximum isometric force (MIF). Stimulated MIF for individuals with SCI is typically assumed to be approximately 50% of the values exhibited by able-bodied muscles, which itself varies between studies and individuals. A method for estimating subject-specific MIF during dynamic motions in individuals with SCI produced by electrical stimulation has been developed to test this assumption and obtained more accurate estimates for biomechanical analysis and controller design. A simple on-off controller was applied to individuals with SCI seated in the workspace of a motion capture system to record joint angles of three types of trunk motions: forward flexion, left and right lateral bending followed by returning, un-aided, to upright posture via neural stimulation delivered to activate the muscles of the hips and trunk. System identification was used with a musculoskeletal model to find the optimal MIF values that reproduced the experimentally observed motions. Experiments with five volunteers with SCI indicate that an MIF of the 50% able-bodied values commonly used is significantly lower than the identified estimates in 33 of 44 muscle groups tested. This suggests that the strengths of paralyzed muscles when stimulated with FNS have been underestimated in many situations and their true force outputs may be higher than the values

Musa L. Audu, mxa93@case.edu.

Authors' contributions AB: Planned and executed the experiments and simulations. Drafted the manuscript.
LL: Prepared the subjects for experiments, profiled the subjects for best baseline and saturation muscle stimulation levels, spotted the subjects during the experiments, and offered invaluable suggestions of controller settings.
AF: Helped with the design and implementation of the experiments.
RJT: Coordinated the implantation of the subjects and provided overall administrative and academic supervision for the whole project.
MLA: Designed the self-righting control system, helped with planning and execution of the experiments, and coordinated the overall work.

Ethical approval All procedures performed in studies involving human participants were in accordance with the ethical standards of the institutional and/or national research committee (Louis Stokes Cleveland Veterans Affairs Medical Center IRB #07101-H36) and with the 1964 Helsinki declaration and its later amendments or comparable ethical standards.

Competing interests All authors declare no competing interests in this work.

Publisher's note Springer Nature remains neutral with regard to jurisdictional claims in published maps and institutional affiliations.

suggested for use in simulation studies with musculoskeletal models. These findings indicate that subject-specific musculoskeletal models can more closely mimic the motions of subjects by using individualized estimates of MIF, which may allow the design and tuning of controllers while reducing the time spent with subjects in the loop.

Keywords

Trunk control; Seated balance; Functional neuromuscular stimulation (FNS); Spinal cord injury (SCI); Maximum isometric force (MIF)

1 Introduction

One of the most significant losses for people with spinal cord injury (SCI) is their ability to maintain trunk stability. Trunk stability is the ability for people to keep their torso upright without using their upper extremities or external surfaces for support. Anderson [1] polled individuals with paraplegia and tetraplegia about what the highest priority in functional restoration should be after an injury. In both populations, trunk stability was ranked third, highlighting its significance to persons with SCI.

Functional neuromuscular stimulation (FNS) is an intervention that can be applied to excite the nerves that innervate the trunk and hip muscles that are vital for pelvic and spinal posture and maintaining trunk stability [2–4]. However, delivery of FNS must be achieved via well-defined control schemes; the development of which in turn requires extensive exploration of several musculoskeletal parameters for the individual subjects. This is because SCI affects people in entirely different ways, including the response to stimulation, thereby requiring that each individual has specific controller design parameters. Therefore, design of control systems for maintaining trunk stability requires extensive tuning experiments with the subjects. Musculoskeletal models that have been carefully created to be as anatomically realistic as possible with respect to the specific subject can greatly reduce the extent of these tuning experiments. Considering the versatility of musculoskeletal models and the availability of accurate model development software such as OpenSim [5], the design of stimulation control systems for trunk stability can be accelerated. Anatomic realism can be achieved by ensuring that the skeletal and muscular characteristics of the model are as close as possible to those of the subject under study.

The important muscular parameters for Hill-type muscle models [6] commonly used in musculoskeletal simulations are as follows: the optimum fiber length, the tendon slack length, the pennation angle, and the maximum isometric force (MIF), which is the maximum force that a muscle can produce when it is maximally excited with its length held fixed. The MIF is one of the parameters that is most affected by paralysis and has a more pronounced impact on the overall force-production capacity of the muscle [7].

Currently, the main method for estimating the MIF is to multiply the physiological cross-sectional area (PCSA) with the specific tension. The PCSA is the cross-sectional area of the muscle in the plane perpendicular to the fibers at the thickest part of the muscle and the specific tension is a measure of intrinsic muscle strength that normalizes MIF to PCSA [8].

Although this method of calculating the MIF is rather straight forward, the estimate can be an inaccurate measure of MIF for a specific individual. This is because the methods of estimating both the PCSA and the specific tension have a high uncertainty in themselves. The traditional method for estimating PCSA is performed by harvesting and measuring muscle areas from cadavers [9, 10] or more recently, by imaging studies using MRI [11]. The main disadvantage of the cadaveric approach is that the harvested tissue is not an ideal representation of the live muscles because the characteristics of the muscle change during contraction [8]. The estimated specific tension, which should be the same for all muscles, has been shown to vary substantially from 62 [12] to 155 kN/m^2 [8] based on in vivo testing.

There also exist experimental techniques for estimating MIF in able-bodied as well as SCI individuals [13]. One popular method involves rigidly strapping the body segments on either side of a joint in a dynamometer machine such as the Biodex (Biodex Medical Systems, Inc., Shirley, NY), with the joint axis aligned with the rotational axis of the dynamometer. The subject is then asked to make maximum voluntary contractions of the muscles crossing that joint, or in the case of SCI, maximally stimulating some or all the individual muscles crossing the joint while keeping the segments rigidly fixed in place. This allows for isometric measurements of muscle strength often in terms of the joint moment. The MIF is then estimated by dividing the maximum moment with the estimated moment arm of the muscle or muscles. Using this static approach, Garner and Pandy [14] described a method for in vivo estimation of peak isometric force in muscles of able-bodied subjects using optimization. In that study, a nested optimization minimized the error between torque-angle curves of maximally contracted muscles with the torque-angle curves generated by a musculoskeletal model to get estimates for the MIF for each muscle involved. Optimization of the MIF values may also be a technique for estimating the MIF for a subject performing dynamic actions.

Dynamic optimizations have been shown to produce estimates of the muscle strengths required to execute an activity that are similar to static estimates. In a study by Morrow et al., the muscle forces required during wheelchair propulsion were optimized in a static and dynamic environment using a musculoskeletal model [15]. For all optimized muscles, there was a 9.9% global root-mean-squared error (RMSE) between the static and optimized estimates, which suggests that they are in good agreement. Anderson and Pandy [16] performed a similar comparison between static and dynamic optimization of gait and found an even greater similarity between the two outputs, going so far as to claim that they are “practically equivalent.”

The dynamometry method works well for joints such as the elbows, hips, knees, and ankles that typically join two clearly identified body segments. However, the method does not work well for trunk muscles which cross several spinal segments that are difficult to isolate. Keeping the trunk in a static pose during testing can also be challenging without highly elaborate equipment. In such situations where muscle actions are distributed simultaneously over numerous joints, dynamic measurement may serve as a better approach for estimating the MIF.

For people with SCI, the MIF for some lower extremity muscles are assumed to be 30–50% of able-bodied values based on the maximum joint torque produced when the paralyzed muscle is completely activated with neural stimulation [17]. Using this as a guide, many previous musculoskeletal modeling studies [18–20] have been developed based on the assumption that the MIF of stimulated paralyzed muscles is of the order of 50% of that for able-bodied individuals. While this may hold true for some muscles, others may have substantially different values, and the differences may further be exacerbated by other individual variations due to the individual effects of the injury.

Considering the importance of MIF in musculoskeletal modeling, especially for people with paralysis, more accurate estimates of MIF for individual subjects are desired. With better MIF estimates, the models can become more realistic, which can lead to faster development of functioning stimulus controllers and improved neuroprosthesis performance. The objective of this work is to report on a new approach to obtain more accurate measures of MIF for hip and trunk muscle groups activated with FNS by matching the trajectories of the trunk obtained in constraint-free motion experiments with those generated by a three-dimensional subject-specific musculoskeletal model actuated by equivalent realistic Hill-type musculotendon elements.

2 Methods

2.1 Participants

Five volunteers with SCI at different thoracic and cervical levels who lacked volitional trunk control participated in the study. Table 1 lists their anthropometric and neurological characteristics. Each of the volunteers was implanted with intramuscular, epimysial, or nerve cuff electrodes to excite the motor nerves of hip and back muscles as listed in the last column of Table 1. All experiments were conducted by activating the nerves of the paralyzed muscles with the implanted electrodes which were sometimes augmented by surface stimulation to ensure complete muscle recruitment or to access muscles not part of the implanted systems. All participants signed the consent form approved by the local institutional review board before participating in the experiments.

2.2 Experimental setup

Volunteers sat in their own wheelchairs, which were placed in the work volume of a 16-camera motion capture system (Vicon Motion Systems Ltd., Oxford, UK). A schematic of the experimental setup is shown in Fig. 1. A wireless sensor containing a CMA3000-D01 accelerometer (VTI Technologies, Vantaa, Finland) and CC430F6137IRGC microcontroller (Texas Instruments, Dallas, TX) was taped to the back of the subject around the posterior spinal process of the T1 vertebra to measure tilt of the trunk in the sagittal and coronal planes representing trunk flexion/extension (sagittal plane) and trunk lateral bending (coronal plane). An external control unit (ECU) allowed for feedback and modulation of the stimulation signals sent to the implanted and surface electrodes based on the readings from the tilt sensor [21].

Retro-reflective markers were taped to the skin at the left and right anterior- and posterior-superior iliac spines, shoulders, and on top of the T1 tilt sensor. Others were attached laterally on the thighs, arms (elbows, upper-arm, forearms, wrists), a headband, and on the wheelchair. With these markers, it was possible to compute the total trunk angle in the coronal and sagittal planes. Motion capture data were recorded at 100 Hz.

2.3 Experimental procedure

In the experiments, the input variable to the musculotendon elements was the stimulation pulse width (PW) to the nerves serving the paralyzed muscles. With the subject sitting quietly upright, the muscles were kept at baseline stimulation levels to ensure a stable erect seated posture. These baseline stimulation levels were generally kept at 0 μs unless the subject was unable to sit upright without contracting the muscle, in which case these baseline values ranged between 0 and 50 μs as necessary to ensure an erect posture. Throughout, stimulation was controlled via a MATLAB Simulink program running in the xPC Host-Target real-time control environment [22]. The tilt sensor signal was sampled at 40 Hz and stimulation was applied at 20 Hz.

The subject was asked to use volitional upper extremity effort to commence moving the trunk in the desired direction (forward, rightward, or leftward) and, once started, to let the trunk continue to tilt under the action of gravity alone without further voluntary input. As soon as the trunk tilt exceeded a value set by a “flexion threshold” (OF in Fig. 1), appropriate muscles were maximally stimulated to return the trunk to the erect position. The maximum stimulation PW varied between 50 and 250 μs depending on the subject and the muscles required to complete the motion. Once the trunk tilt crossed another “extension threshold” (OE in Fig. 1), close to the erect posture, stimulation was reduced to the baseline level appropriate for the original erect posture [23]. The pulse amplitudes were chosen based on the individual responses of the implanted muscles and were kept constant during experiments for each individual. Trials were captured with the trunk moving either forward in the sagittal plane or to the right or to the left in the coronal plane. A spotter was always present to ensure the subject did not fall in case the stimulus was insufficient or was not triggered. A pulse signal from the real-time xPC Target computer synchronized the beginning and end of a trial with the Vicon motion capture system.

For each subject, a total of 3 to 5 trials were captured. In each trial, the subject leaned in the forward, left, or right directions 2 times for a maximum of 6 cycles per trial. In each trial, the order of directions was randomly assigned. There was a 3–5-s interval between each cycle and a 5–10-min rest between each trial to allow the muscles to recover. Sometimes the subject was not able to recover fully to an erect position and had to be helped by the spotter to return to erect. Such cycles were removed from the analysis.

For each experiment, the trunk pitch (sagittal) and trunk bend (coronal) angles were calculated from the Vicon motion capture data recorded while the subject returned to the upright posture. The muscle activation profiles during each trial and the corresponding trunk joint angles were stored for use as inputs to the stimulation component. The joint angle data was resampled to match the 20-Hz stimulation PW data for use in the simulation component of the study.

2.4 Computer simulation component

The height and weight for each subject were used along with anthropometric tables to generate skeletal models scaled to match the individuals' bone segments and joints. The tables were based on studies of anthropometry and segment inertial parameters from the Naval Biodynamics Lab [24] and De Leva [25]. The overall musculoskeletal models were created in the OpenSim/SIMM software (National Center for Simulation in Rehabilitation Research/Musculographics, Inc) modeling environments with each model consisting of 13 joints, 13 bone segments, and 36 Hill-type muscle elements which encompass the pelvis, trunk, and upper extremities in a seated posture [20]. The 36 muscle elements represent the muscle groups which are either directly or indirectly affected by a stimulus pulse provided by the implanted or surface electrodes.

Table 2 shows the tested muscle groups for each subject in the study. In particular, we arranged the muscles into groups as follows: Trunk Benders [lumbar Erector Spinae (ES), Quadratus Lumborum (QL) and External Obliques (ES)], Trunk Extensors (ES), Hip Adductors [posterior Adductor Magnus (AM)], Hip Flexors [Iliopsoas (IP), Rectus Femoris (RF)], Hip Extensors [3 branches of Gluteus Maximus (GX)], and Hamstrings [Semimembranosus (SM), Semitendinosus (ST) and Biceps Femoris (BF)]. Each group contained muscles that provide similar functions when stimulated and that are anatomically near the implanted muscles. The suggested groupings were used to account for the possibility of stimulation spillover and co-activation of the muscles neighboring the primary target [26, 27]. The Hamstrings and Hip Adductor groups mostly function as hip extensors because the thighs were firmly secured to the wheelchair with a lap belt. Each muscle group corresponds with an implanted electrode, and accounts for any spillover that may result from it.

A system identification method was designed that utilizes the musculoskeletal models along with the activations and joint angles from the experimental procedure to estimate optimal values of MIF for the electrically activated muscles. In the identification simulations, the maximum stimuli applied to the muscles were scaled to the maximum activation levels of the muscles in the model and served as the model inputs; the model outputs were the resultant trunk angles. The total trunk pitch was further sub-divided into its pelvic pitch and lumbar pitch components according to a synergy termed the lumbo-pelvic rhythm [28]. In the lumbo-pelvic rhythm, the approximate formula most commonly used to relate pelvic to lumbar contributions to trunk position is [29]:

$$\frac{Lumbar \quad Pitch}{Pelvic \quad Pitch} \approx 2.2 \tag{1}$$

Thus the 3 angles (pelvic pitch, lumbar pitch, and lumbar bend) serve as the outputs from the musculoskeletal model.

Forward simulations were conducted with the musculoskeletal model in an optimization loop generating the 3 joint angle outputs as a function of the stimulus input while the MIF was varied. In the optimization, the objective function was the square root of the residual sum of squares (RSS) between the simulated joint angles from the model and the actual joint

angles from the experimental trials. A genetic algorithm (GA) code-named SOGA (single-objective genetic algorithm) which is a part of the JEGA library [30] from the DAKOTA package [31] was used to minimize the objective function. The optimization problem was solved using the parallel cluster at the CWRU High Performance Computing Facility. The overall identification cycle is depicted in Fig. 2.

Equation 2 shows the objective function, $J_D(x)$, for each direction that the subject could lean. The objective values for all lean directions are then summed together into a total objective function, $J_{total}(x)$, as indicated in Eq. 3.

$$J_D(x) = \sqrt{\sum_{i=1}^{n} \left[\left(x_S^i - x_E^i\right)^2_{\text{pitch,P}} + \left(x_S^i - x_E^i\right)^2_{\text{pitch,L}} + \left(x_S^i - x_E^i\right)^2_{\text{bend,L}} \right]} \quad (2)$$

With n as the number of time intervals for the trial, x as the joint angles, subscript S as simulation, subscript E as experimental, P as pelvic component, and L as lumbar component. The subscript D indicates the direction which varied between forward, left, and right.

$$J_{\text{total}}(x) = J_{\text{forward}}(x) + J_{\text{left}}(x) + J_{\text{right}}(x) \quad (3)$$

The total objective function is the sum of the objective functions in all three directions: forward flexion, left, and right lateral bending. The total objective function uses one experimental cycle in each lean direction. These cycles are chosen randomly from the set of cycles collected during the experimental trials.

The GA minimized the total objective function with the MIF for each muscle as the decision variables. The optimization determined the MIF values for each active muscle that would result in a minimization of the objective function. Each trial of the system identification required the input of the actual activations and joint angles from a trial in each direction. To ensure mainly the effect of stimulation is processed, the cycle breakdown of a typical experimental trial run through the system identification was as follows: 1% before the stimulation turns on, 49.5% when stimulation is active, and 49.5% after stimulation ends as depicted in Fig. 3. The muscle groups included in the optimization are outlined in Table 2, which lists the muscles that make up each grouping as well as the stimulation status for each subject. The optimization was stopped when any of three set criteria were satisfied. These were as follows: (1) the number of function evaluations exceeded 100,000, (2) the number of iterations exceeded 1000, and (3) changes in successive objective function values were less than a small number (set at 1.0e–3). Most of the optimization runs were stopped primarily to satisfaction of condition 3, and occasionally to condition 2.

2.5 Statistical analyses

Single-sample 2-sided t test comparisons were carried out to test the alternative hypothesis that the mean values of the identified MIF for each subject/direction differ from the commonly used 50% able-bodied values. The Shapiro-Wilk tests for normality were conducted for the mean MIF calculated over all cycles in a given direction. Significant

values were set at $p < 0.05$. All statistical analyses presented were based on individual subject data.

To quantify the difference between the experimental and simulated joint angles, we computed the normalized root-mean-squared error (NRMSE), a metric expressing the average deviation of the simulated joint angles from the experimental joint angles as a percentage of the range of the experimental values for the condition (ex. pelvic pitch and forward lean). It is computed as the square root of the average squared difference between the measured and estimated (model) signals, divided by the range of the measured, multiplied by 100. That is:

$$\mathrm{NRMSE} = \left(\frac{\mathrm{RMSE}}{X_{\mathrm{mea,max}} - X_{\mathrm{mea,min}}}\right) \cdot 100 \tag{4}$$

Where

$$\mathrm{RMSE} = \sqrt{\frac{\sum_{i=1}^{n} \left(X_{\mathrm{mea},i} - X_{\mathrm{mod},i}\right)^2}{n}} \tag{5}$$

In these equations, $X_{\mathrm{mea},i}$ and $X_{\mathrm{mod},i}$ are the ith entries in the measured and estimated (model) variable signals, respectively, n is the number of frames in each of the two signals, and $X_{\mathrm{mea,max}}$ and $X_{\mathrm{mea,min}}$ are respectively the maximum and minimum entries in the measured signal.

3 Results

Figure 4 a–c show typical joint angle outputs from the simulations of the data for subject S-2 compared with the equivalent experimental results in all three directions of leaning. The experimental joint angles (blue) were the input to the identification procedure, and the simulated joint angles (red) were output from the model following the exit from the optimization loop. The difference between the simulation joint angles and the experimental joint angles was minimized in the optimization as described in the minimization of Eq. 3. The plotted lines are the means of 5 or more trials, and the dashed lines are 1 standard deviation from the mean. These plots depict the typical output for each subject following the system identification procedure. The scales for the plots in each direction were kept the same so that the differences in magnitude can be compared across joint angles. From Fig. 4 a for the forward leaning direction, the most prominent angles are the pelvic and lumbar pitch angles, with the lumbar bend angle remaining low, at around ± 7.5°. As expected, forward trunk flexion primarily involves muscles acting in the sagittal plane with minimal involvement of those responsible for lateral bending. On the other hand, from Fig. 4 b and c for the left and right lateral bending, the bend angles are more prominent. There are also smaller magnitude changes in the pelvic and lumbar pitch angles, which imply that most sideways movements are accompanied by some small forward movements of the trunk since the trunk is dynamically moving without restraint.

The NRMSE for the means for each subject and for all movement directions are summarized in Table 3. Each column in the table contains the NRMSE value for each of the three joint

angles in the average motion of 5 or more trials: pelvic pitch, lumbar pitch, and lumbar bend. The number of cycles used to analyze the data for the subject/direction is shown in parenthesis under each direction label. The Shapiro-Wilk tests for normality yielded p values greater than 0.05 (minimum $p = 0.13$) for all directions except two—subjects S4 and S5, Right Lean direction ($p = 0.04$ and $p = 0.04$, respectively). The NRMSE is below 33% when simulating the prominent joint angles, except for the left lumbar bend of subject S-4, with 12 of the 15 columns (5 subjects, 3 directions) having the smallest NRMSE in these prominent joint angle combinations (pitches and forward lean, bends, and lateral bending). The pelvic and lumbar pitch in forward lean and the lumbar bend in both left and right lateral bending should be expected to have the largest magnitude, as the motions are in their respective planes.

All three directions were optimized at the same time, meaning the MIF estimates consider the motion in all three directions. The prominent combinations were the ones with the smallest NRMSE in 12 of the 15 columns of Table 3, suggesting that the optimization algorithm in most cases was able to minimize the difference in the prominent combinations. In the comparisons where the change in magnitude is smaller, the higher NRMSE could be explained by random variations within the individual cycles.

The final outcomes from the system identification were the MIF estimates for the 12 bilateral muscle groups, which are shown in Fig. 5 a and b for all 5 subjects. Figure 5 a displays the estimates for the left muscle groups and Fig. 5 b displays the estimates for the right muscle groups. The mean MIF estimates (in Newton) for each muscle group and their error bars (± 1 standard deviation) are plotted side-by-side with the 50% able-bodied estimates typically adopted for musculoskeletal modeling after SCI. If a subject did not have one of the muscle groups stimulated during the experiments, the estimate bar is left blank for that muscle group. Figure 5 a and b also contains significance bars and asterisks ($p < 0.05$) for single-sample 2-sided t test comparisons between the 50% able-bodied MIF values and the means of the identified MIF values for each subject. The p values from these t tests are shown in Table 4.

Of the 44 muscle groups estimated over 5 subjects, 33 of the estimates were significantly greater than the 50% able-bodied estimate ($p < 0.05$) using this two-sided t test. With a higher degree of significance ($p < 0.01$), the number of significantly different MIF values is reduced to 22. Up to 50% of the muscle groups still showed significant differences in the MIF values between the value estimated from able-bodied quantities and the ones determined by the subject-specific identification process.

4 Discussion

MIF estimates currently used in musculoskeletal modeling for SCI are based entirely on assumptions about the relative strength of SCI muscles to able-bodied muscles. Able-bodied estimates of MIF themselves also vary substantially depending on the method used. This paper outlines estimates for SCI muscles of the trunk and hip that are subject-specific and can be used in place of the assumed values when designing musculoskeletal models for the

subjects tested, allowing for models that will be able to more properly mimic the stimulated motions of these subjects.

Initial analysis with individual implanted muscles alone resulted in unusually high MIF estimates, pointing to the possibility that stimulation was spilling over to other neural structures, resulting in co-activation of synergistic muscles that provided additional force. To accommodate the potential for co-activation or spillover to multiple muscles, the muscle groupings in Table 3 were chosen instead of using only the muscle targeted for activation in the musculoskeletal model. During the experiments, there may have been some spillover from the stimulated nerves which lead to the innervation of surrounding muscles [26, 27]. In the case of the spillover in these trials, the additional muscles are synergistic, so they would likely also act in the same direction as intended. This addition of muscle groups also addressees the assumption that the targeted muscle is the one that is activated, when it could be a combination of synergistic muscles functioning together. The suggested muscle groupings consider the muscles which are most likely to receive spillover stimulation due to the proximity of their innervating nerve branches. By comparing the whole group rather than only the individual muscle targeted for activation, the effects of spillover should be more accurately accounted for in the results.

The able-bodied MIF values were calculated by multiplying the specific tension specified in Wilkenfeld et al. [32] with the PCSA of the muscles of the gluteus maximus, upper legs [9], and lumbar trunk [11]. In the current study, 75% of the muscle groups resulted in MIF values that were statistically significantly larger than the common assumption that the MIF for SCI muscles are around 50% of able-bodied values. This suggests that using such an assumption for the force-generating capabilities of stimulated muscles after SCI could lead to an underestimation of the values in general.

The methods of estimating able-bodied MIF by multiplying PCSAwith specific tension are themselves associated with a lot of uncertainty, both in the PCSA values and in the values of specific tension. In the optimizations conducted by Garner and Pandy with able-bodied subjects [14], the PCSA values obtained were generally larger than the values from the literature. In addition, the PCSA value for the same muscle could vary substantially depending on the method of estimation [33]. Delp et al. [10] inspected cadavers to describe the anatomy of lumbar muscles (quadratus lumborum, erector spinae, rectus abdominus) and predict their moment generating capacities. The values for the PCSA reported were smaller than values found using imaging techniques like those completed by Tracy et al. [11]. Similarly, the specific tension, the other component of MIF, also has a rather large variance in its possible values. In vivo tests [8] and simulations [34] show that specific tension has been found to lie anywhere between 62 and 155 kN/m^2. As a result, the MIF variance for able-bodied values is even greater.

Calculating model parameters like MIF via a musculoskeletal model requires that the model itself is robust enough to be insensitive to slight changes in the model parameters. Were the model too sensitive, there would likely be large variations in the estimates and the results would be difficult to trust. Valente et al. [35] examined the robustness of subject-specific musculoskeletal models to see how they responded to uncertainties in parameter

identification. That study showed that the uncertainties in parameter identification only have a moderate effect on model predictions, and that there were no crucial parameters required for model estimation. Although the study was inconclusive about the robustness of the model, it did find that there was a low probability for the uncertainty to be on the same magnitude as the output values, suggesting that calculating model parameters using the musculoskeletal model can be an effective technique. That study, however, was performed with a musculoskeletal model in gait, meaning the number of degrees of freedom was higher than compared with our study.

The 50% assumption that has been commonly applied appears to be smaller than is required to represent the muscle outputs for the individuals with SCI participating in this study. With the results of the current study, it is possible to create an estimate which is a function of able-bodied values for MIF and more closely matches the identified MIF values. An estimate of 65% of the able-bodied value is much closer to matching the identified values displayed in Fig. 5 a, b resulting from the experiments described. If this estimate is used, the number of significantly ($p < 0.05$) different MIF estimate values is reduced substantially: only 14 of the 44 muscle groups, compared with 33 of 44 with the 50% estimate.

There are several limitations in the current study. The musculoskeletal model utilized in the system identification is based on the work of Lambrecht et al. [20], which has several assumptions that are also present in the current study. One such assumption is that the pelvis does not rotate in the coronal plane during lateral bending movements of the trunk. This was implemented experimentally by strapping the thighs to the chair. Despite these efforts, there is still a possibility that there was some amount of pelvic roll that was unaccounted for in the results. Another limitation is that muscle fatigue was not accounted for within the model. To minimize the effects of fatigue in the experiments, the subjects were given ample time to rest (5 min) between trials and used only a few (3–5) cycles of trunk movement in each trial.

A third limitation, which is common in the solving of most optimization problems, is the potential of landing in a local rather than a global minimum. In the current study, several optimization algorithms were considered such as pattern search and gradient descent. In the final analysis we chose to use a genetic algorithm because it has a much higher potential to find a global minimum with a large search space while also reaching a solution relatively quickly [36].

One final limitation that may have had an impact on the results is the time following implantation. The users had a variable amount of time with the implant before the beginning of this study that ranged from 2 to 20 years. It is possible that the time spent using an implanted FNS system may have an impact on the MIF when compared with typical SCI subjects without access to a means to stimulate.

5 Conclusions

We estimated the MIF of trunk and hip muscles for 5 subjects with implanted neuroprosthesis systems through dynamic optimizations of a musculoskeletal model. These estimates were greater than the 30–50% able-bodied values typically assumed in previous

musculoskeletal modeling studies. With these subject-specific estimates, future musculoskeletal modeling work can be more subject-specific. This may allow for tuning and testing of controllers in simulation that will reduce the need of testing with subjects in the loop. With improved controllers, the functionality and performance of implanted neuroprostheses can continue to be improved.

The results of the current study also support the feasibility of using system identification of a musculoskeletal model to estimate the MIF values for the paralyzed muscles of individuals SCI. Adapting this technique of dynamic optimization to other model parameters is an area of continuing investigation.

Acknowledgments

The authors would like to acknowledge the contributions of our study participants, the Motion Study Laboratory at the Louis Stokes Cleveland Veterans Affairs Medical Center, and the Cleveland APT Center. This work also made use of the High-Performance Computing Resource in the Core Facility for Advanced Research Computing at Case Western Reserve University.

Funding information This material was based on work supported in part by the National Institutes of Health (Grant 1R01NS101043-01) and the Department of Defense, SCIR Program (Grant W81XWH-17-1-0240).

Biographies

Akhil R. Bheemreddy received the B.S. Degree in biomedical engineering with a focus in biomechanics and completed the M.S. Degree in biomedical engineering from Case Western Reserve University, Cleveland OH, USA in 2019. He is currently working as a research engineer at the Kessler Foundation in West Orange, NJ, USA.

Aidan R. W. Friederich received B.S. degrees in mechanical engineering and biomedical engineering from Colorado State University, Fort Colins, CO, USA. He is currently pursuing a doctorate in biomedical engineering from Case Western Reserve University, Cleveland OH, USA.

Lisa M. Lombardo received the B.S. degree in Psychology from The Ohio State University, Columbus, Ohio, USA, the Master's degree in Physical Therapy from Slippery Rock University, Slippery Rock, PA, USA.

Ronald J. Triolo (S '78, M '86) received a BS in Electrical Engineering from Villanova University, Villanova PA in 1980, and MS degrees in both Biomedical Engineering and Electrical Engineering from Drexel University in Philadelphia PA in 1982 and 1984, respectively, as well as a doctorate in Biomedical Engineering for the design and clinical testing of an actively powered and myoelectrically controlled above knee prosthesis for transfemoral amputees in 1986. Dr. Triolo was Director of Research at the Philadelphia Unit of Shriners Hospitals from 1986 through 1994 he where he investigated neuroprosthetic and neurotherapeutic uses of neural stimulation for children with motor dysfunction due to spinal cord injury or cerebral palsy. Dr. Triolo is currently a Tenured Full Professor of Biomedical Engineering at Case Western Reserve University and a Senior Research Career Scientist with the Rehabilitation Research & Development Service of the US Department of Veterans Affairs. He is the Executive Director of the Advanced Platform Technology Center of the Department of Veterans Affairs where he oversees the design, prototyping and production of novel medical devices for the rehabilitation of individuals with sensorimotor impairments or limb loss. He also directs the Motion Study Laboratory of the Louis Stokes Cleveland Department of Veterans Affairs Medical Center where he pursues research in the development and clinical application of neuroprostheses and restorative technologies, biomechanics and the control of movement, rehabilitation engineering, and the assessment of assistive technology. Dr. Triolo has authored over 125 peer-reviewed publications and currently leads independent research programs funded the NIH, DoD and other federal and private agencies to restore or enhance the upright and seated mobility, posture, balance, and universal access for individuals with neuro-musculo-skeletal disorders.

Musa L. Audu received the B.E. and M.E. degrees in mechanical engineering from Ahmadu Bello University, Zaria, Nigeria, and the Ph.D. degree in mechanical engineering with a major in biomechanics from Case Western Reserve University, Cleveland, OH, USA. He was an Associate Professor of Mechanical Engineering at Abubakar Tafawa Balewa University, Bauchi, Nigeria, and the Rector (President) of the Federal Polytechnic. He is currently Principal Investigator with the Cleveland Advanced Platform Technology Center and Research Professor in the Department of Biomedical Engineering, Case Western Reserve University. His current research interests include applications of musculoskeletal

modeling, simulation of dynamic systems, and optimal control of biomechanical systems. Dr. Audu is a member of the American Society of Biomechanics and the International Functional Electrical Stimulation Society.

Abbreviations

SCI	Spinal cord injury
FNS	Functional neuromuscular stimulation
MIF	Maximum isometric force
PCSA	Physiological cross-sectional area
PW	Pulse width
GA	Genetic algorithm
RSS	Residual sum of squares
NRMSE	Normalized root-mean-squared error
ECU	External control unit

References

1. Anderson KD (2004) Targeting recovery: priorities of the spinal cord-injured population. J Neurotrauma 21(10):1371–1383 [PubMed: 15672628]
2. Park ES, Park CI, Lee HJ, Cho YS (2001) The effect of electrical stimulation on the trunk control in young children with spastic diplegic cerebral palsy. J Korean Med Sci 16(3):347–350 [PubMed: 11410698]
3. Triolo RJ, Boggs L, Miller ME, Nemunaitis G, Nagy J, Bailey SN (2009) Implanted electrical stimulation of the trunk for seated postural stability and function after cervical spinal cord injury: a single case study. Arch Phys Med Rehabil 90(2):340–347 [PubMed: 19236990]
4. Vanoncini M, Holderbaum W, Andrews BJ (2012) Electrical stimulation for trunk control in paraplegia: a feasibility study. Control Eng Pract 20(12):1247–1258
5. Seth A, Sherman M, Reinbolt JA, Delp SL (2011) OpenSim: a musculoskeletal modeling and simulation framework for in silico investigations and exchange. Procedia IUTAM 2:212–232 [PubMed: 25893160]
6. Scovil CY, Ronsky JL (2006) Sensitivity of a Hill-based muscle model to perturbations in model parameters. J Biomech 39(11): 2055–2063 [PubMed: 16084520]
7. Gföhler M, Lugner P (2004) Dynamic simulation of FES cycling: influence of individual parameters. IEEE Trans Neural Syst Rehabil Eng 12(4):398–405 [PubMed: 15614995]
8. Maganaris CN, Baltzopoulos V, Ball D, Sargeant AJ (2001) In vivo specific tension of human skeletal muscle. J Appl Physiol 90:865–872 [PubMed: 11181594]
9. Friedrich JA, Brand RA (1990) Muscle fiber architecture in the human lower limb. J Biomechanics 23(1):91–95
10. Delp SL, Suryanarayana S, Murray WM, Uhir J, Triolo RJ (2001) Architecture of the rectus abdominis, quadratus lumborum, and erector spinae. J Biomech 34:371–375 [PubMed: 11182129]
11. Tracy MF, Gibson MJ, Szypryt EP, Rutherford A, Corlett EN (1989) The geometry of the muscles of the lumbar spine determined by magnetic resonance imaging. Spine 14(2):186–193 [PubMed: 2922639]

12. Ikai M, Fukunaga T (1968) Calculation of muscle strength per unit cross-sectional area of human muscle by means of ultrasonic measurement. Int Z Angew Physiol Einschl Arbeitsphysiol 26:26–32
13. Sisto SA, Dyson-Hudson T (2007) Dynamometry testing in spinal cord injury. J Rehabil Res Dev 44(1):123–136 [PubMed: 17551866]
14. Garner BA, Pandy MG (2003) Estimation of musculotendon properties in the human upper limb. Ann Biomed Eng 31:207–220 [PubMed: 12627828]
15. Morrow MM, Rankin JW, Neptune RR, Kaufman KR (2014) A comparison of static and dynamic optimization muscle force predictions during wheelchair propulsion. J Biomech 47(14):3459–3465 [PubMed: 25282075]
16. Anderson FC, Pandy MG (2001) Static and dynamic optimization solutions for gait are practically equivalent. J Biomech 34:153–161 [PubMed: 11165278]
17. Kobetic R, Marsolais EB, Miller PC (1994) Function and strength of electrically stimulated hip flexor muscles in paraplegia. IEEE Transactions of Rehabilitation Engineering 2(1):11–17
18. Heilman BP, Audu ML, Kirsch RF, Triolo RJ (2006) Selection of an optimal muscle set for a 16-channel standing neuroprosthesis using a human musculoskeletal model. J Rehabil Res Dev 43(2):273–286 [PubMed: 16847793]
19. Gartman SJ, Audu ML, Kirsh RF, Triolo RJ (2008) Selection of optimal muscle set for 16-channel standing neuroprosthesis. J Rehabil Res Dev 45(7):1007–1017 [PubMed: 19165690]
20. Lambrecht JM, Audu ML, Triolo RJ, Kirsch RF (2009) Musculoskeletal model of trunk and hips for development of seated posture-control neuroprosthesis. J Rehabil Res Dev 46:515–528 [PubMed: 19882486]
21. Trier SC, Buckett JR, Campean A, Miller ME, Montague FW, Vrabec TL, Weisgarber JA (2001) A modular external control unit for functional electrical stimulation. In: Proceedings of the 6th Annual Conference of the International Functional Electrical Stimulation Society. International Functional Electrical Stimulation Society, Cleveland, p 109
22. (2007) xPC target selecting hardware guide. The MathWorks Inc. Available via Mathworks. https://www.mathworks.com/tagteam/37937_xpc_target_selecting_hardware_guide.pdf
23. Murphy JO, Audu ML, Lombardo LM, Foglyano KM, Triolo RJ (2014) Feasibility of closed-loop controller for righting seated posture after spinal cord injury. J Rehabil Res Dev 51(5):747–760 [PubMed: 25333890]
24. (1988) Military male aviators. In: Anthropometry and mass distribution for human analogues. Naval Biodynamics Laboratory. Available via Humanics. https://www.humanics-es.com/ADA304353.pdf
25. De Leva P (1996) Adjustments to Zatsiorsky-Seluyanov's segment inertia parameters. J Biomech 29(9):1223–1230 [PubMed: 8872282]
26. Triolo RJ, Liu MQ, Kobetic R, Uhlir J (2001) Selectivity of intramuscular electrodes in the lower limbs. J Rehabil Res Dev 38(5): 533–544 [PubMed: 11732831]
27. Quiring DP, Warfel JH (1967) The head, neck, and trunk: muscles and motor points, 3rd edn. Lea & Febiger, Philadelphia
28. Vazirian M, Van Dillen L, Bazrgari B (2016) Lumbopelvic rhythm during trunk motion in the sagittal plane: a review of the kinematic measurement methods and characterization approaches. Phys Ther Rehabil 3:5 [PubMed: 29034099]
29. Serber H (1994) The study of lumbar motion in seating In: Lueder R, Noro K (eds) Hard facts about soft machines: the ergonomics of seating. Taylor & Francis, Pennsylvania, pp 423–431
30. Eddy J, Lewis K (2001) Effective generation of Pareto sets using genetic programming. In: Proceedings of ASME Design Engineering Technical Conference. American Society of Mechanical Engineers, New York
31. Adams BM, Bauman LE, Bohnhoff WJ, Dalbey KR, Ebeida MS, Eddy JP, Eldred MS, Hough PD, Hu KT, Jakeman JD, Stephens JA, Swiler LP, Vigil DM, and Wildey TM, DAKOTA, A. Multilevel parallel object-oriented framework for design optimization, parameter estimation, uncertainty quantification, and sensitivity analysis: version 6.8 user's manual, 5 2018

32. Wilkenfeld AJ, Audu ML, Triolo RJ (2006) Feasibility of functional electrical stimulation for control of seated posture after spinal cord injury: a simulation study. J Rehabil Res Dev 43(2):139–152 [PubMed: 16847781]

33. Brand RA, Pedersen DR, Friederich JA (1986) The sensitivity of muscle force predictions to changes in physiologic cross-sectional area. J Biomech 19(8):589–596 [PubMed: 3771581]

34. Burkhart KA, Bruno AG, Bouxsein ML, Bean JF, Anderson DE (2018) Estimating apparent maximum muscle stress of trunk extensor muscles in older adults using subject-specific musculoskeletal models. J Orthop Res 36(1):498–505 [PubMed: 28597988]

35. Valente G, Pitto L, Testi D, Seth A, Delp SL, Stagni R, Viceconti M, Taddei F (2014) Are subject-specific musculoskeletal models robust to the uncertainties in parameter identification? PLoS One 9(11):e112625 [PubMed: 25390896]

36. Nowaková J, Pokorný M (2014) System identification using genetic algorithms In: Kömer P, Abraham A, Snášel V (eds) Proceedings of the Fifth International Conference on Innovations in Bio-Inspired Computing and Applications IBICA 2014, Advances in intelligent systems and computing, vol 303 Springer, Cham, pp 413–418

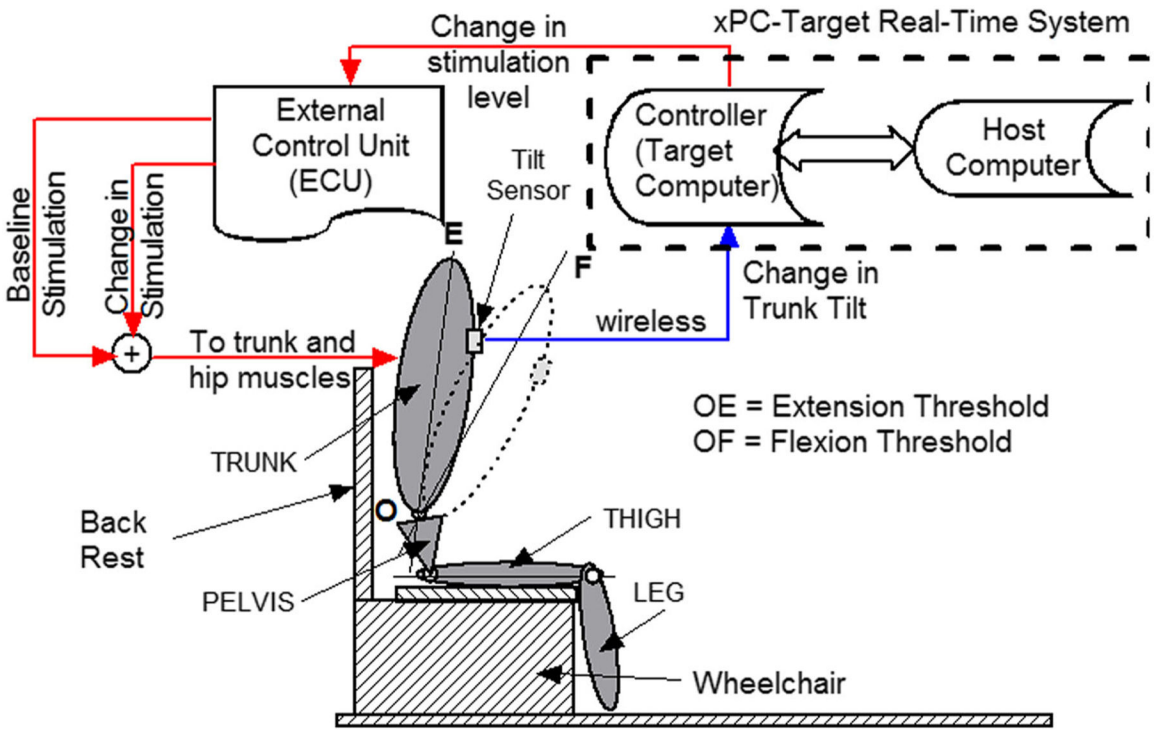

Fig. 1.

Schematic of trunk self-righting control system showing subject seated in work volume of motion capture cameras. Two computers (target and host) manage the real-time environment for the experiments. Settings for the tilt sensor are defined as OE for the extension threshold and OF for the flexion threshold. Experiments were conducted with trunk tilt in the sagittal and coronal planes. The ECU generates the stimulation inputs to the implanted and surface electrodes, which are modulated depending on the signal from the tilt sensor. The xPC host-target environment allowed for real-time control during the experiment

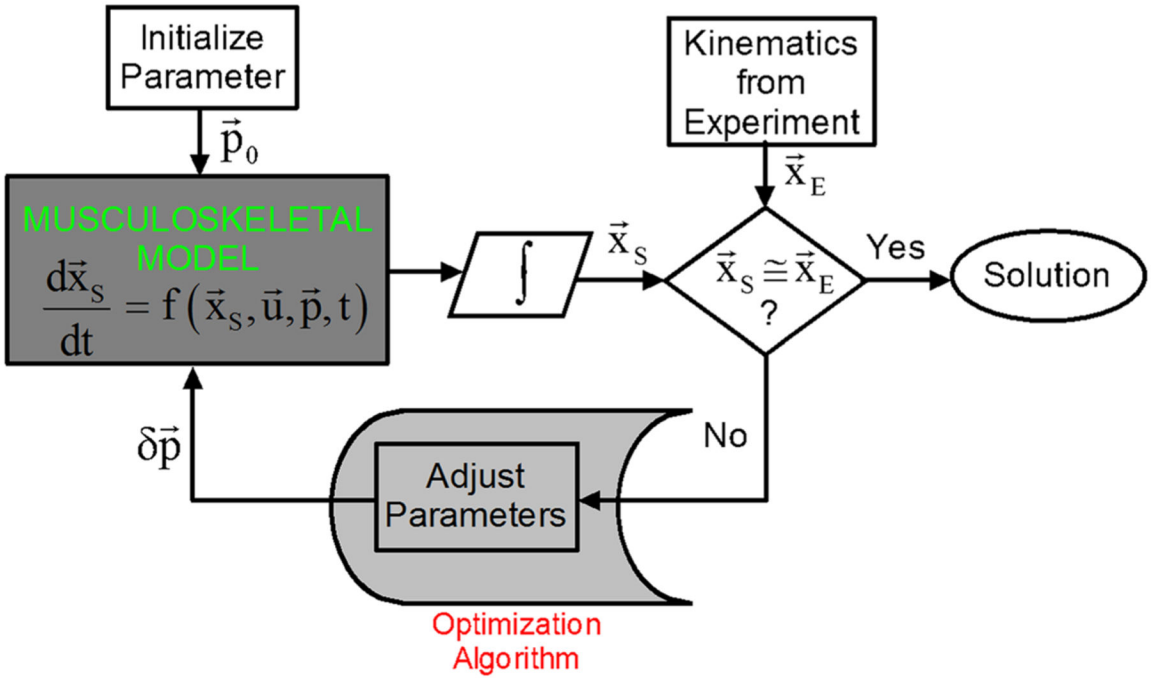

Fig. 2.

The optimization loop in the computer simulation component. A genetic algorithm is used as the optimization algorithm. X_S represents the kinematics from the simulation and X_E represents the kinematics from the experiments. Once the exit condition is reached, the solution outputs the MIF estimates and final kinematics from the musculoskeletal model

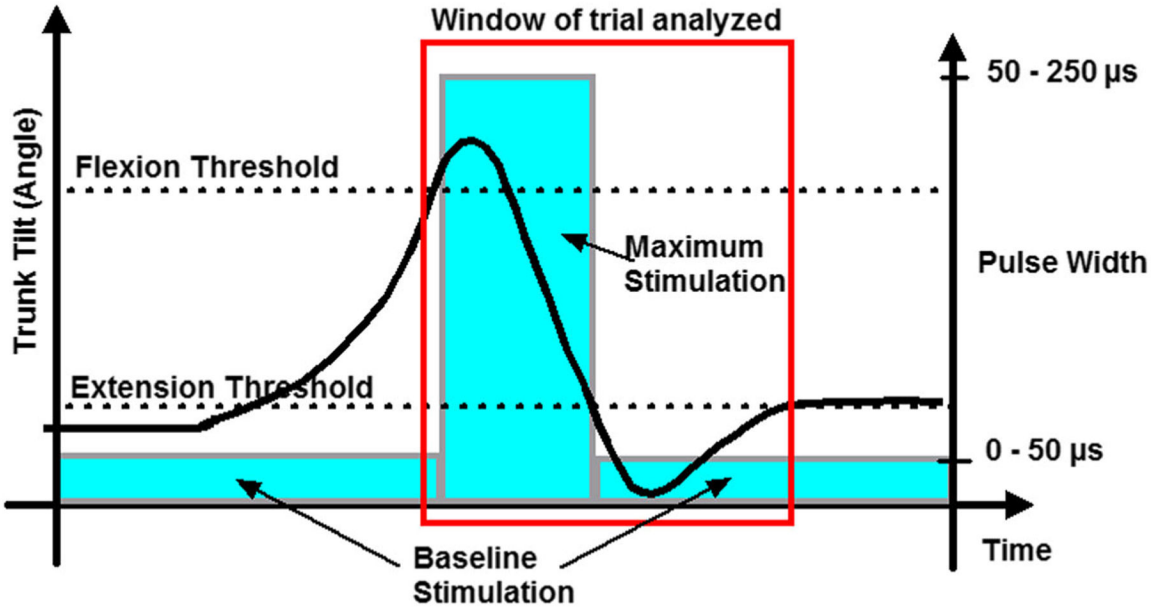

Fig. 3.

Typical variation of trunk tilt as a function of time (not to scale). With trunk supported in erect posture with baseline stimulation, it starts to fall freely until the flexion threshold is reached. Thereafter, maximum stimulation is applied which arrests the fall and starts to return the trunk toward erect. Maximum stimulation varies between 50 and 250 µs depending on the subject and muscle. Once tilt returns to the extension threshold, baseline stimulation is resumed. Portions covered by red box depict the portion of the trial being analyzed (a cycle). The cycle makeup is 1% before maximum stimulation is applied, 49.5% during maximum stimulation, and 49.5% after maximum stimulation

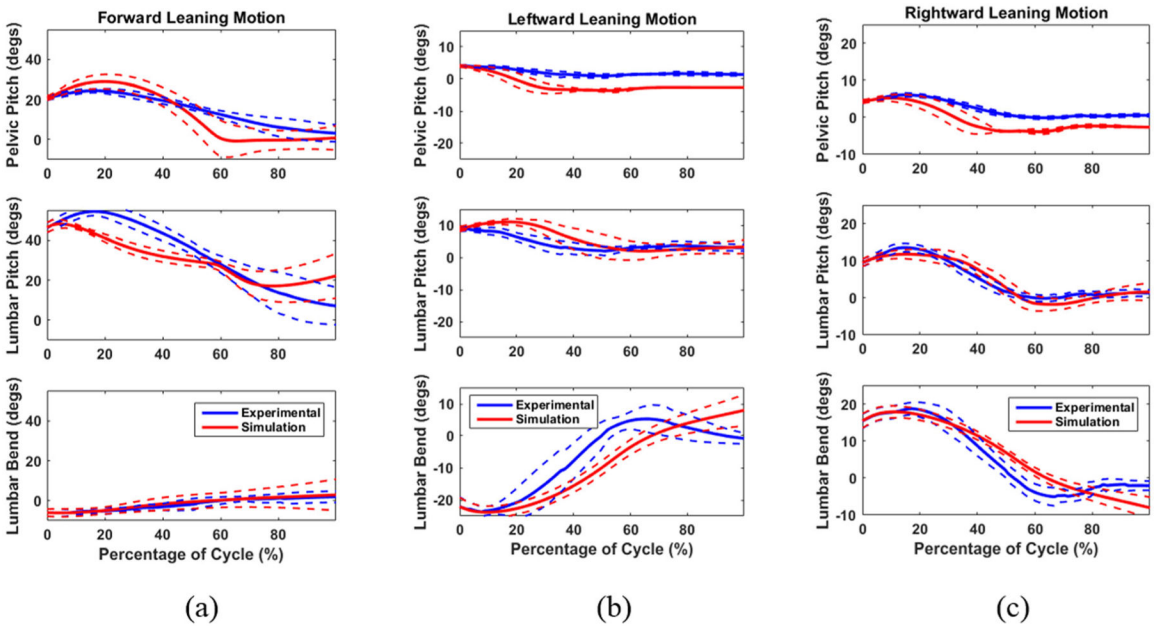

Fig. 4.

Plots of the joint angle outputs from S-2 in all three directions of lean: **a** Forward flexion in the sagittal plane ($N = 14$), and **b** leftward lateral bending ($N = 13$) and **c** rightward lateral bending ($N = 10$) in the coronal plane. The three joint angles are pelvic pitch, lumbar pitch, and lumbar bend. The blue lines are the means of the joint angle from the experimental trials and the red lines are the results from the simulation. The dashed lines are 1 standard deviation from the means

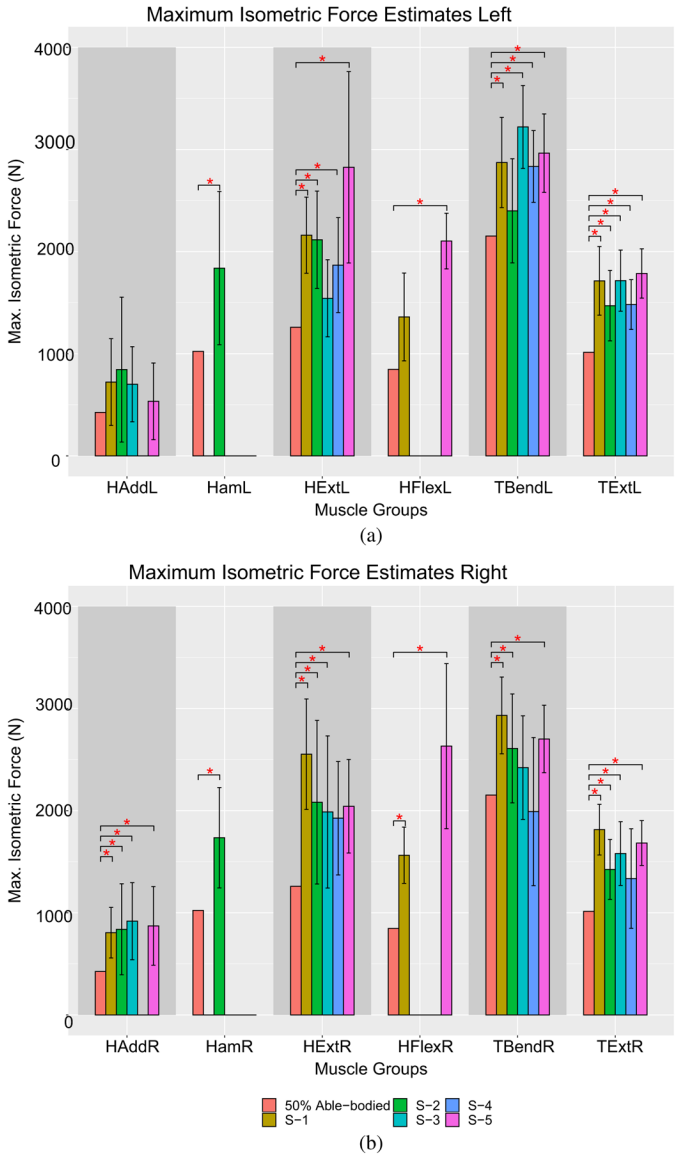

Fig. 5.

Maximum isometric force (MIF) estimates for each subject compared with the 50% able-bodied estimate for each muscle group on the **a** left and **b** right. Error bars are given for each identified value. For subjects that do not have a certain muscle group stimulated, the MIF estimate is blank. Significance bars and asterisks are shown which indicate the significance of the difference from the identified values with the 50% able-bodied estimates are shown ($p < 0.05$)

Table 1

Summary of clinical characteristics of participants in this study

Subject	Age	Gender	Height (cm)	Weight (kg)	Injury level	AIS grade+	Time post injury[a] (y)	Time post implant[a] (y)	Muscles stimulated
S-1	43	F	175.3	82.8	T4	A	6.8	4.1	ES, QL, GX, AM, IP
S-2	47	F	175.3	57.6	C7	B	20.8	19.1	ES, QL, GX, AM, SM
S-3	28	M	185.4	52.6	C5	C	7.9	2.5	ES, QL, GX, AM
S-4	28	M	188	81.6	C5	A	29	8.2	ES, QL, GX
S-5	50	M	172.7	71.7	T3	A	2.3	1.5	ES, QL, GX, AM, IP

AM posterior portion of Adductor Magnus, *ES* lumbar Erector Spinae, *GX* Gluteus Maximus, *GM* Gluteus Medius, *QL* Quadratus Lumborum, *IP* Ilipsoas, *SM* Semimembranosus, +*A* motor and sensory complete, *B* motor complete with sensory sparing, C motor and sensory incomplete

[a]At time of testing

Med Biol Eng Comput. Author manuscript; available in PMC 2021 April 01.

Table 2

The muscle groupings used in the maximum isometric force estimates (MIF). These groupings account for any situation spillover that would otherwise be ignored by the model. The columns corresponding to each subject indicate whether the muscle groups were included in the stimulation during the experiment

Muscle group	Included muscles	S-1	S-2	S-3	S-4	S-5
Trunk Benders	Quadratus Lumborum, Erector Spinae, External Obliques (all lumbar)	Included	Included	Included	Included	Included
Trunk Extensors	Erector Spinae (lumbar)	Included	Included	Included	Included	Included
Hip Adductors	Adductor Magnus (posterior)	Included	Included	Included		Included
Hip Flexors	Iliopsoas (Iliacus and Psoas), Rectus Femoris	Included				Included
Hip Extensors	Gluteus Maximus (3 heads)	Included	Included	Included	Included	Included
Hamstrings	Semimembranosus, Semitendinosus, Biceps Femoris		Included			

Med Biol Eng Comput. Author manuscript; available in PMC 2021 April 01.

Table 3

The normalized root-mean-squared error (NRMSE) for each joint angle and direction for all subjects. The simulation result was compared with the experimental joint angles. Number in parenthesis under each direction label is the number of cycles used for the analysis. The NRMSE is normalized by dividing the root-mean-squared error by the range for each comparison then multiplying by 100 to make a percentage. It was calculated by comparing the means of the simulated trials with the means of the experimental trials. A NRMSE closer to zero means that the simulation result is closer to the experimentally measured data. The value is a measure of the deviation between the simulation joint angles and the experimental joint angles as a percentage of the range of experimental values

Normalized root-mean-squared error (% of experimental range)															
	S-1			**S-2**			**S-3**			**S-4**			**S-5**		
	Forward lean (17)	**Left lean (12)**	**Right lean (9)**	**Forward lean (14)**	**Left lean (13)**	**Right lean (10)**	**Forward lean (16)**	**Left lean (15)**	**Right lean (13)**	**Forward lean (14)**	**Left lean (9)**	**Right lean (8)**	**Forward lean (12)**	**Left lean (11)**	**Right lean (8)**
Pelvic pitch	19.72	86.36	96.55	28.33	125.63	52.47	23.70	76.69	104.61	30.69	39.85	45.20	8.24	31.32	33.44
Lumbar pitch	12.74	52.36	52.74	18.59	37.02	9.91	13.71	36.39	51.12	15.27	15.14	33.35	18.49	22.60	31.39
Lumbar bend	28.66	32.19	21.60	9.32	20.20	14.02	45.10	22.50	18.04	117.83	42.76	11.70	18.91	19.85	22.12

Table 4

The p values for the comparison between the identified MIF values and the 50% able-bodied values using a two-tailed t test for each muscle group. If the muscle group is not active for a subject, the corresponding cell is a left blank. The cells are shaded in if $p < 0.05$

***p* values for identified MIF vs. 50% able-bodied**					
Muscle groups	**S-1**	**S-2**	**S-3**	**S-4**	**S-5**
Left Trunk Benders	0.0220	0.2137	0.0001	0.0124	0.0014
Left Trunk Extensors	0.0096	0.0072	0.0003	0.0128	0.0001
Left Hip Adductors	0.1921	0.1386	0.0711		0.4729
Left Hip Flexors	0.0559				0.0000
Left Hip Extensors	0.0057	0.0014	0.0711	0.0430	0.0045
Left Hamstrings		0.0180			
Right Trunk Benders	0.0097	0.0461	0.1179	0.6438	0.0046
Right Trunk Extensors	0.0019	0.0055	0.0014	0.2147	0.0002
Right Hip Adductors	0.0264	0.0344	0.0078		0.0220
Right Hip Flexors	0.0043				0.0011
Right Hip Extensors	0.0059	0.0228	0.0279	0.0549	0.0040
Right Hamstrings		0.0046			